Optogenetic inhibition of chemically induced hypersynchronized bursting in mice.

Berglind, Fredrik; Ledri, Marco; Sørensen, Andreas Toft; Nikitidou, Litsa; Melis, Miriam; Bielefeld, Pascal; Kirik, Deniz; Deisseroth, Karl; Andersson, My; Kokaia, Merab

Published in:
Neurobiology of Disease

DOI:
10.1016/j.nbd.2014.01.015

2014

Optogenetic inhibition of chemically induced hypersynchronized bursting in mice

Abbreviated title: Optogenetic inhibition of induced bursting in mice

Fredrik Berglind[1], Marco Ledri[1*], Andreas Toft Sørensen[1#], Litsa Nikitidou[1*], Miriam Melis[1§], Pascal Bielefeld[1†], Deniz Kirik[2], Karl Deisseroth[3], My Andersson[1] and Merab Kokaia[1]

Affiliations: 1. Experimental Epilepsy Group, Epilepsy Center, Department of Clinical Sciences, Lund University, SE-22184 Lund, Sweden 2. Brain Repair and Imaging in Neural Systems (BRAINS) Unit, Department of Experimental Medical Sciences, Lund University, SE-22184 Lund, Sweden 3. Dept of Bioengineering, Stanford University, 94305 Stanford, CA, USA.

Corresponding author: Merab Kokaia, Experimental Epilepsy Group, Epilepsy Center, Department of Clinical Sciences, BMC A11, Lund University Hospital, SE-22184 Lund, Sweden. Email: merab.kokaia@med.lu.se Telephone: +46 46 2220547

Number of pages: 30 (including figures and tables)
Number of figures, tables, multimedia and 3D models: 5 figures, 3 tables
Number of words for Abstract, Introduction, and Discussion: Abstract: 187, Introduction: 353, Discussion: 904

Present addresses: * Institute of Experimental Medicine, Hungarian Academy of Sciences, 1083 Budapest, Hungary; # McGovern Institute for Brain Research, Massachusetts Institute of Technology, 02139 Cambridge, MA, USA; § Department of Neuroscience "B.B. Brodie", University of Cagliari, Cittadella di Monserrat, SS554 bivio per Sestu, Monserrato, Italy; † Swammerdam Institute for Life Sciences, Amsterdam University, 1098 XH Amsterdam, The Netherlands.

Funding for the research was provided by: the Swedish Research Council, the Swedish Brain Foundation, the Nanometer Structure Consortium at Lund University, the Thorsten and Elsa Segerfalk Foundation, the Johan and Greta Kock Foundation, the Royal Physiographic Society in Lund.

The funding agencies had no role in any element of planning, data collection, analysis or writing of this research paper.
The authors declare no competing financial interests.

Abstract

Synchronized activity is common during various physiological operations but can culminate in seizures and consequently in epilepsy in pathological hyperexcitable conditions in the brain. Many types of seizures are not possible to control and impose significant disability for patients with epilepsy. Such intractable epilepsy cases are often associated with degeneration of inhibitory interneurons in the cortical areas resulting in impaired inhibitory drive onto the principal neurons. Recently emerging optogenetic technique has been proposed as an alternative approach to control such seizures but whether it may be effective in situations where inhibitory processes in the brain are compromised has not been addressed. Here we used pharmacological and optogenetic techniques to block inhibitory neurotransmission and induce epileptiform activity *in vitro* and *in vivo*. We demonstrate that NpHR-based optogenetic hyperpolarization and thereby inactivation of a principal neuronal population in the hippocampus is effectively attenuating seizure activity caused by disconnected network inhibition both *in vitro* and *in vivo*. Our data suggest that epileptiform activity in the hippocampus caused by impaired inhibition may be controlled by optogenetic silencing of principal neurons and potentially can be developed as an alternative treatment for epilepsy.

Keywords

Epileptiform, Seizure, Optogenetics, Mouse, GABA, Picrotoxin, Bicuculline, Inhibition, NpHR, Hippocampus

Introduction

Epilepsy is a heterogeneous chronic neurological disorder with a prevalence of up to 1% in the general population (Duncan et al., 2006; Sander, 2003). While drug treatment is successful in a majority of cases, certain types of epilepsies are not as easily controlled. About 30-40% of patients with one of the most common forms of epilepsy, temporal lobe epilepsy (TLE), are drug resistant (Duncan et al., 2006; Engel, 2001). This puts demand on developing alternative treatment strategies.

It has been proposed that epileptic seizures could be the result of synchronization of principal cells by interneurons (Avoli and de Curtis, 2011; Isomura et al., 2008) through activation of $GABA_A$ receptors. However, both experimental models and human temporal epilepsies are often associated with degeneration or dysfunction of various inhibitory interneuron populations (de Lanerolle et al., 1989; Malmgren and Thom, 2012; Morimoto and Goddard, 1986; Zhang and Buckmaster, 2009). This is believed to significantly reduce inhibitory drive on pyramidal neurons and thereby promote hyperexcitability and seizures (Kumar and Buckmaster, 2006; Morimoto, 1989; Zhang and Buckmaster, 2009). Additional support for this assumption comes from experimental data showing induction of epileptiform activity, both *in vitro* and *in vivo,* by application of $GABA_A$ receptor antagonists (Hwa et al., 1991; Miles and Wong, 1983; Piredda et al., 1985; Strombom et al., 1979) indicating that one of the main consequences of inhibitory interneuron degeneration leading to seizures is decreased $GABA_A$ receptor-mediated inhibition in the epileptic network. We have previously demonstrated that optogenetic hyperpolarization (Zhang et al., 2007) of principal neurons by light-induced activation of NpHR (Halorhodopsin) can counteract synchronized epileptiform activity generated by electrical stimulation when GABAergic transmission in the hippocampus is not compromised (Tonnesen et al., 2009). We now

hypothesized that in a scenario where interneuron inhibitory function is compromised by blockade of $GABA_A$ receptors, resulting in epileptiform activity presumably driven by principal cells, hyperpolarization of these cells by optogenetic approach would be strong enough to stop epileptiform activity. Indeed, we demonstrate that epileptiform bursting in the hippocampus induced by $GABA_A$ receptor antagonists is attenuated by hyperpolarization of principal neurons using an optogenetic strategy both *in vitro* and *in vivo*.

Materials and Methods

Animals and Surgery

Female FVB mice (Charles River) were housed according to local animal house standards with 12-hour light/dark cycles and food & water *ad libitum*. All procedures followed ethical permits approved by the Malmö/Lund Animal Research Ethics Board. Animals were anaesthetized with 1.5-2.5% isoflurane (4% at induction) (Isofluran, Baxter), 0.5 mL bupivacaine (Marcain, AstraZeneca) was used as local anesthetic and Chlorhexidine (Fresenius Kabi) was used for wound cleaning. During and after surgery, physiological saline (0.5 mL) was injected subcutaneously to maintain hydration.

Induction of status epilepticus

One group of animals used in the *in vitro* study were weighed and injected subcutaneously with kainic acid (KA) at a dose of 30 mg per kg of body weight, diluted in sterile PBS and adjusted to pH 7.2-7.4. Animals were monitored for 3 hours after injection and behavioural seizures were scored according to a modified Racine scale (Racine, 1972): grade 0, arrest, normal behaviour; grade 1, facial twitches (nose, lips, eyes); grade 2, chewing, head nodding; grade 3, forelimb clonus; grade 4, rearing, falling

on forelimbs; grade 5, imbalance and falling on side or back; grade 6, status epilepticus. If animals did not develop behavioural seizures in the first 20 minutes after the first injection, they were subjected to a second injection of half the initial dose. All KA mice used in the study displayed at least four grade 5 generalized seizures.

Viral vector injection

Stereotactic injections with 1 µL AAV5-hSyn-eNpHR3.0-YFP vector were made on mice of 4-5 weeks age into the ventro-posterior hippocampus, at AP-3.2, ML-3.1 from bregma, DV-3.6 and -3.2 from dura (0.5 µL each depth, 0.1 µL/min). For the KA group, injection was made 4-5 weeks after KA treatment. Virus was produced in-house as described previously (Ledri et al., 2012), and the titer was 5.4×10^{12}. Animals were anaesthetized and placed in a stereotactic frame (Kopf Instruments), bupivacaine was injected into the skin of the skull before a midline incision was made. Connective tissue was removed by scraping and applying a small amount of 3% hydrogen peroxide. A small burr hole was drilled at the coordinates stated and the dura was carefully punctured using a thin (27G) bent hypodermic needle. A pulled glass capillary (Stoelting, cat. # 50613 or Drummond Scientific, cat. # 1-000-0500) fitted to a 5 µL Hamilton syringe with generic polyolefin heat-shrink tube was then lowered to the target depths and used for injection of the viral vector. The wound was cleaned and closed with tissue glue (Histoacryl, B.Braun) or resorbing thread (Ethicon).

In vitro slice preparation and electrophysiology

Three to five weeks after virus injection, animals were briefly anesthetized and decapitated. The brain was quickly removed and immersed in chilled sucrose-based cutting solution containing (in mM): sucrose 75, NaCl 67, $NaHCO_3$ 26, glucose 25, KCl 2.5,

NaH_2PO_4 1.25, $CaCl_2$ 0.5, $MgCl_2$ 7 (pH 7.4, osmolarity 305-310 mOsm). Horizontal slices containing the hippocampus and entorhinal cortex (300 µm thickness) were prepared essentially as previously described (Ledri et al., 2012). After cutting, slices were incubated in sucrose-based solution for 15-30 minutes at 34°C, and then transferred to an incubation chamber containing artificial cerebrospinal fluid (aCSF) at room temperature. The composition of aCSF for incubation and recording was as follows (in mM): NaCl 119, $NaHCO_3$ 26, glucose 25, KCl 2.5, NaH_2PO_4 1.25, $CaCl_2$ 2.5 and $MgSO_4$ 1.3 (pH 7.4, osmolarity 305-310 mOsm). All solutions were constantly oxygenated with carbogen (95% O_2, 5% CO_2).

For electrophysiological recordings, individual slices were transferred to a submerged recording chamber, constantly perfused with oxygenated aCSF and maintained at 32 °C. Recording pipettes were pulled from thick-walled borosilicate glass with a Flaming-Brown horizontal puller (P-97, Sutter Instruments, CA) and contained aCSF for field recordings (1-3 MOhm tip resistance), or (in mM): K-Gluconate 122.5, KCl 12.5, KOH-HEPES 10, KOH-EGTA 0.2, MgATP 2, Na_3GTP 0.3, NaCl 8 (pH 7.2-7.4, mOsm 300-310, 3-5 MOhm tip resistance) for whole-cell patch clamp experiments.

Epileptiform activity in the slices was induced by perfusion with Mg^{2+}-free aCSF containing 50 µM 4-aminopyridine (4-AP) and 100 µM Picrotoxin (PTX). Field recordings were performed from the pyramidal layer of area CA3 of the hippocampus, and whole-cell experiments were performed from CA3 pyramidal cells. In certain cases, field and whole-cell-recordings were performed simultaneously. Slices (n = 9, 8 & 6) were accumulated from 4, 3 and 3 animals for Naïve, KA and Control group, respectively, with 2-5 repeat measurements for each slice. Infrared differential interference contrast microscopy was used as a visual guide for the approach of the recording pipettes. For whole-cell recordings, biocytin (3-5 mg/ml) was routinely added to the pipette solution

on the day of the recording. Uncompensated series resistance (typically 8-30 MΩ) was constantly monitored via -5 mV voltage steps and recordings were discontinued after changes of >20% or if the resting membrane potential of the cells reached values more positive than -50 mV. Data were sampled at 10 kHz with an EPC-10 amplifier (HEKA Elektronik, Lambrecht, Germany) and stored on a G4 Macintosh computer with PatchMaster software (HEKA) for offline analysis.

Orange-yellow light was generated by a mercury light bulb filtered by a 593 ±40 nm brightline excitation filter cube (Senrock) and was applied through the microscope lenses. After recordings, slices were fixed overnight in 4% PFA in PB and subsequently stored in Walter's antifreeze solution (ethylene glycol and glycerol in PB, pH 7.0-7.4, VWR) at -20 °C. All chemicals and drugs used were from Sigma-Aldrich, unless indicated otherwise.

Chemical optrode & laser

Three components make up the chemical optrode (Fig. 3A): a 200 µm core, 37 NA multimode optic fiber (BFL37-200, Thorlabs) with a FC/PC connector; a 2 inch 1 MΩ tungsten microelectrode (0.127 mm ø shaft, 1 µm ø tip, parylene-C coated, cat. # TM21A10, WPI UK) and a borosilicate glass capillary (0.58 mm inner ø, 1 mm outer ø, cat. # 1B100F-6, WPI UK) pulled on a Model P-1000 pipette puller (Sutter Instruments). The pipette tip was smoothed on a grinder and microforge (EG-44/MF-830, Narishige). The fiber was cut using a diamond pen (Thorlabs), coating was stripped within ~1.5 cm of the tip and the fiber was then glued to the microelectrode so that the electrode tip protruded 0.4-0.6 mm from the fiber tip. The glued optrode was inserted through a cut 200 µL plastic pipette tip (Eppendorf) and secured with generic blu-tac for increased stability, the glass micropipette was then attached with blu-tac to the plastic pipette, so

that the tip comes in close vicinity to the electrode tip and the assembly secured by applying heated sticky wax (see fig. 3A). Each optrode was calibrated for the input light power needed to achieve maximum tolerated emission power at the fiber tip (75 mW mm^{-2} (Cardin et al., 2010); 2.3 mW output for a 200 μm fiber). The optic fiber was connected to a 593 nm yellow-orange laser with 25 mW power supply (CrystaLaser), light emission was measured with a 1916-C power meter (Newport).

In vivo experimental procedure

Three months after viral injection mice were again anaesthetized, placed in a stereotactic frame, the same AP and ML coordinates used for viral injections were located, where a burr hole was opened and the chemical optrode was lowered into the brain to DV-3.0 (electrode tip, measured from dura), controlled by a MO-10 manual micromanipulator (Narishige) attached to the stereotax. The glass capillary of the chemical optrode had been prefilled with 3 mM bicuculline methiodide (BM, Ascent Scientific) in PBS, with 2 mg/ml biocytin, and attached by tubing to a Picospritzer IID air-pressure microinjection system (General Valve Corporation).

An EP1 Ag/AgCl reference eletrode (WPI UK) was placed under the skin at the skull base. Local field potential (LFP) recording using a DP-311 amplifier (Warner Instruments), filters set to HP at 0.1 Hz and LP at 3k Hz, commenced at 10 kHz sample rate on a Powerlab 4/35 acquisition system (AD Instruments) connected to a Windows laptop PC with LabChart Pro software (AD Instruments). For multiunit activity recording, the signal was bandpass filtered at 300-3k Hz in the software. A custom-built copper mesh faraday cage was placed over the setup during recording, and the stereotax was resting on a vibration isolation platform (VIP-320, WPI UK).

The optrode was left in place for at least 5 minutes to allow the brain tissue to accommodate and was then lowered in 0.5 mm increments, with a resting period of at least 1 minute in between, while testing the laser effect in 5-10 s periods until a depth was reached where NpHR3.0 activation was deemed appropriate. The laser was operated through the Powerlab system by TTL connection and engaged from within the recording software. Light application on/off markers were automatically incorporated. The end depth was between DV-3.05 and -3.3. Approximately 1.5-3 µL BM solution (end totals) was then injected by activating the picospritzer air pressure in short bursts (50-100ms, 20-21PSI). Typically, one such burst would move the solution ~0.5 µL. The injected volumes are approximate as eyesight was used to determine the movement of the solution meniscus in the capillary, aided by visual markers. Had BM-induced bursting not appeared within 3-4 minutes, another pair of air bursts was given.

The light treatment protocol was initiated when bursting appeared stable, consisting of a light period of 40 s, followed by a period of 80-120 s without light. This was repeated 10-12 times per animal. Burst frequency was stable throughout the experiments in all animals (with one exception) and there was no indication of decreased efficacy of illuminations over time. In one animal, two periods of unstable interrupted bursting occured in the middle and at the end of the trial, whereby two illumination periods were excluded. All other illumination periods were included in the analysis.

The main criteria for inclusion of animals in the experimental group was NpHR expression in the hippocampal neurons as assessed by postmortem analysis of hippocampal slices for YFP fluorescence. Thus, the *in vivo* control group consisted of six animals, where three animals had been subjected to viral injection, but did not display NpHR-YFP expression in the post-mortem analysis. Additionally, these three animals did not display any hyperpolarization and repolarization deflection in the field potential at

light switch-on and switch-off during recording, confirming absence of NpHR expression. The other three control animals had not been injected with viral vector. In other regards, they were subjected to BM injection (1-4 µL) and light treatment similarly to the NpHR3.0-positive group, using light periods of 30 or 60 seconds in length.

Immediately after the end of the light treatment protocol, animals received a terminal dose of sodium pentobarbital (40 mg/kg) and were transcardially perfused with ice-cold 0.9% saline followed by 4% PFA. The brains were removed and post-fixed in 4% PFA overnight before being transferred to 20% sucrose in PB.

Histology

Brains from *in vivo* trials were cut in 30 µm coronal slices on a microtome (Microm, Thermo Scientific). Slices were rinsed in potassium PBS (KPBS) followed by KPBS with 0.25% Triton X-100 (T-KPBS). To visualize biocytin, slices were incubated in Cy3-conjugated streptavidin (Jackson Immunoresearch), 1:400 in T-KPBS for 1.5 hours. Electrophysiological slices were similarly rinsed, then blocked in 5% Normal Goat Serum in T-KPBS and incubated with rabbit anti-GFP primary antibody, 1:10 000 (Abcam, ab290) overnight, rinsed and followed by 2h incubation in FITC-conjugated goat anti-rabbit secondary antibody (1:400, Jackson Immunoresearch). Additionally, biocytin staining was done as described above. To visualize mossy fiber sprouting in KA treated animals, we performed immunohistochemical stainings for Zinc Transporter 3 (ZnT3) (Chi et al., 2008). After fixation, slices from electrophysiological recordings were additionally cryoprotected in PB containing 20% sucrose for 2 days, and then cut in 50 µm sections on a microtome. Staining was performed as above, except the primary antibody was rabbit anti-ZnT3 antibody (1:500, Synaptic Systems, 197 003) and the secondary was Cy3-conjugated. Slices were mounted on glass slides, dried and

coverslipped using 2.5% PVA-DABCO mounting medium with Hoechst-33342 solution (1:1000, Invitrogen) to visualize cell nuclei. Slides were examined in a BX61 microscope fitted with a CCD camera (Olympus) with filters suitable for GFP and Cy3, respectively, and pictures were captured using cellSens Dimension software (Olympus).

Data analysis and statistics

For *in vivo* data, thresholds suitable to the bursting in each animal were set in the cyclic measurements detection tool (two-sided height, detect minimum peak) of the recording software, automatically marking bursts which were then manually screened and approved, adjusted or removed (i.e. artifacts). Minimum interburst distance was set to 1 s. Burst data was extracted using the scope function (including timepoint, coastline, burst duration and max-min amplitude), with scope set to a 1-2 s window (depending on burst characteristics), and then pasted into a spreadsheet (Excel, Microsoft). The amount of bursts in 40 s light periods and corresponding 40 s pre- and post light periods were counted and an average/period was calculated for each animal. For the comparison to control group, period burst data from an animal was normalized to the mean burst count of the pre-light periods in the same animal. In the control group, period lengths were also normalized to 40 s. There were 9-12 periods per animal in the NpHR3.0 group, 3-16 in the control group.

Burst dynamics over the periods was calculated by collecting the timepoints of bursts in pre-, light-, and post periods and sorting them in 4 s bins. A mean was then calculated from the amount of bursts per animal for each bin, and the means were then compared between the last 4 s bin before light and the first 4 s bin after light.

In vitro electrophysiological data was analyzed with FitMaster (HEKA) or Igor Pro 6 (Wavemetrics) softwares. Input resistance values were calculated from the cellular

response to -5 mV test pulses. Action potential (AP) threshold was defined as the point where the fastest rising phase of the first AP in the ramp started. Rheobase was defined as the current needed in the ramp to reach AP threshold. AP amplitude was defined as the difference between the threshold and the peak. AP half-duration was defined as the width of the action potential measured at half amplitude, in ms. For evaluation of light-induced inhibition of epileptiform activity, the frequency of epileptiform bursts in field recordings was analyzed in bins of 30 seconds. Frequency values during light application were compared to values corresponding to periods immediately before and after illumination. Data was normalized to the mean of the 30 s pre-light period, to properly reflect changes compared to control slices. Burst durations were calculated using Minianalysis software v. 6.0.7 (Synaptosoft). Bursts were semi-automatically detected according to individually suited detection settings for each recording and visually validated. Statistical tests and graphing was performed in Prism 5 (GraphPad), α-level = 0.05 used throughout. Statistical tests used were, for paired data: repeated measures ANOVA and paired two-tailed Student's t-test. For unpaired data: one-way ANOVA and Student's t-test (two-tailed) (with Welch's correction, if applicable). Multiple comparisons were done with Tukey's (comparing all pairs) or Bonferroni's (comparing specific pairs) *post hoc* tests. For ANOVA tests, the P value for the omnibus test is stated first, followed by P values for the *post hoc* test comparisons of interest. Traces were visualized in Igor Pro 6 (WaveMetrics). Data is presented as means (Standard Deviation) throughout.

Results

NpHR expression in the hippocampus

The AAV vector construct with the NpHR gene (enhanced version 3.0 (Gradinaru et al., 2010)) and human Synapsin (hSyn) promoter, driving expression in both excitatory and inhibitory neurons (Bogen et al., 2009), was injected into the ventral hippocampus several weeks before *in vitro* or *in vivo* experiments to allow for optimal and widespread transgene expression. The hSyn promoter was chosen to minimize GABA release from interneurons during the light illumination. The expression of NpHR3.0 in the hippocampus was assessed by reporter YFP protein in slices both for electrophysiological recordings *in vitro* and those taken after *in vivo* experiments and was evenly distributed around the injection site in all areas of ventral hippocampus (Fig. 2 (*in vitro*) and 4 (*in vivo*), see further in corresponding sections below), reaching 1.8 mm in dorso-ventral direction and 1.3 mm in anterio-posterior direction.

Epileptiform bursting in vitro

We first investigated whether NpHR3.0 expression could alter neuronal intrinsic electrophysiological properties using whole-cell patch-clamp recordings from CA3 pyramidal neurons of the hippocampus in acute brain slices. We chose the CA3 area because of its high susceptibility to seizure activity among hippocampal areas (Miles and Wong, 1983; Traub and Jefferys, 1994). Membrane properties of cells expressing NpHR3.0 (as confirmed by light-induced photocurrent) were compared to those of CA3 pyramidal neurons from non-expressing control animals. A summary of these data is presented in Table 1, showing no alteration of any of the intrinsic electrophysiological properties, including resting membrane potential, input resistance, action potential

Table 1. Intrinsic membrane properties of CA3 pyramidal cells are not affected by expression of NpHR3.0. Values are means (SD). RMP: Resting Membrane Potential; AP: Action Potential.

	Control (n=6)	**NpHR3 (n=6)**
RMP (mV)	-79.9 (4.6)	-78.8 (3.5)
Input resistance (MΩ)	214.5 (78.5)	289.9(70.4)
AP threshold (mV)	-37.2 (2.3)	-36.3 (2.1)
Rheobase (pA)	297.2 (87.4)	289.9 (30.6)
AP amplitude (mV)	85.6 (4.5)	88.2 (5.2)
AP half duration (ms)	1.1 (0.2)	1.0 (0.1)
Photocurrent (pA)	-	306.1 (221.9)
Light-induced hyperpolarization (mV)	-	24.4 (22.2)

threshold, its amplitude or half-duration, as well as ramp current strength over 500 ms needed to induce APs.

We then investigated whether exposing the NpHR3.0-transfected hippocampal slices to yellow light would suppress epileptiform bursting activity in the CA3 induced by $GABA_A$ receptor blocker PTX (100 μM). To reliably achieve epileptiform bursting of stable frequency, we additionally used Mg^{2+} deprived aCSF containing 50 μM 4-AP, potentiating the effect of PTX. Lowering Mg^{2+} and including 4-AP would enhance glutamatergic transmission by promoting NMDA receptor activation and increasing glutamate release due to broader APs caused by 4-AP (note that $GABA_A$ receptors were already blocked by PTX), which, overall, would be in line with the idea to drive epileptiform network activity predominantly by increased excitatory neurotransmission, while inhibitory neurotransmission is compromised. Epileptiform activity usually appeared within 5-10 minutes, stabilized in frequency after 15-20 minutes and typically remained unaltered for at least 60 minutes. The average frequency of epileptiform bursting was 0.43 (0.12) Hz. Representative recordings from slices subjected to 30 and 60 seconds of light are shown in Figure 1 A & B, respectively.

Figure 1

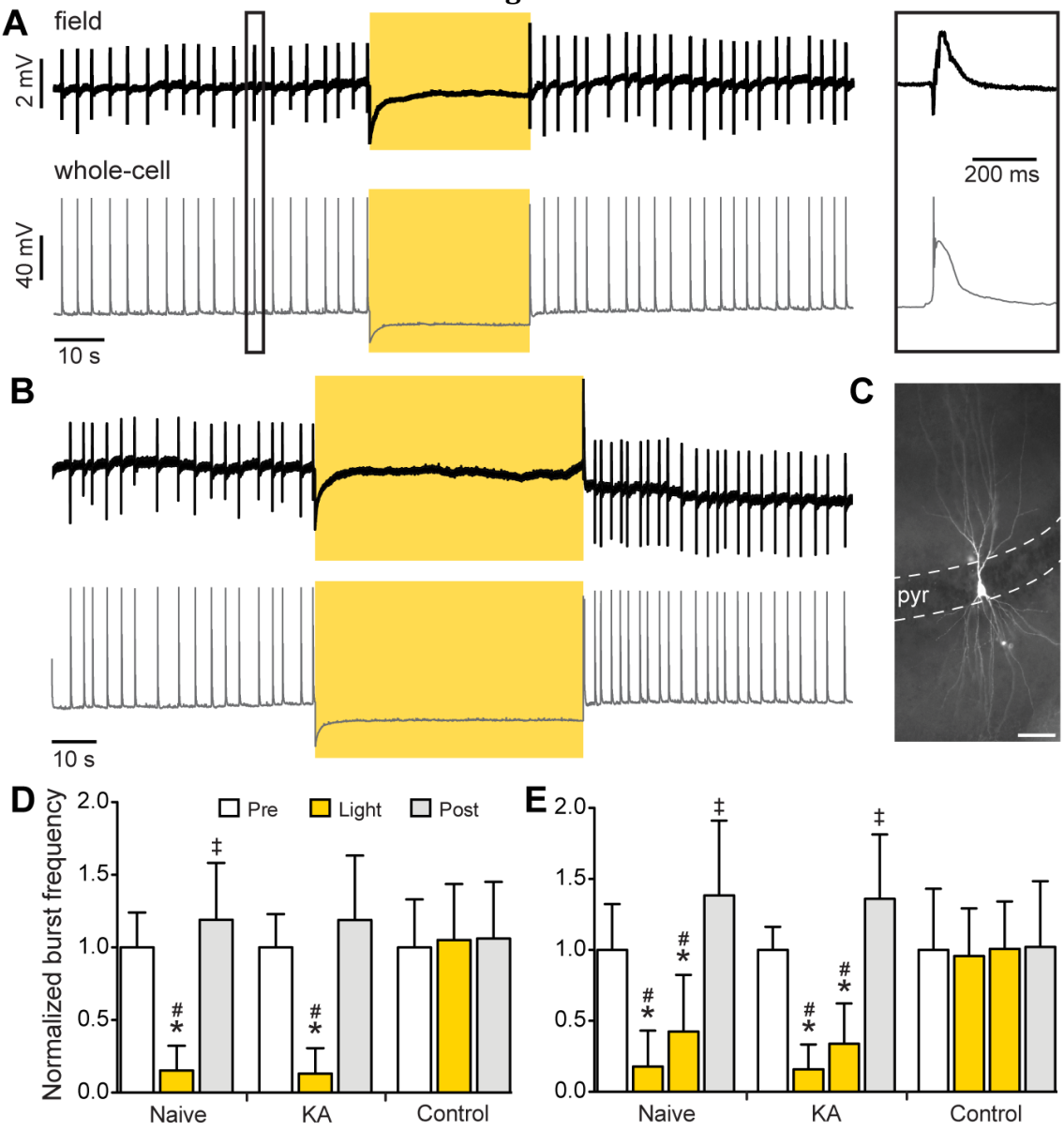

Figure 1 Substantial reduction of PTX induced bursting in acute hippocampal slices from NpHR3.0-expressing mice. **A & B.** Representative recording traces made from the CA3 area of an AAV-NpHR3.0 injected FVB mouse exposed to 30 s (A) and 60 s (B) 593 nm light (yellow boxes) during a simultaneous field and whole-cell recording. The outlined box in A is magnified on the right. **C.** Pyramidal cell of the CA3 filled with biocytin while recording traces in A & B. Pyr: pyramidal cell layer. Scale bar: 100 µm **D & E.** Mean burst frequency of 30 second periods (before, during and after light) normalized to pre-light levels, for acute hippocampal slices from NpHR3.0 expressing animals (Naive (n=9 slices) and KA-injected (n=8)) and non-expressing control animals (n=6), exposed to 30 s (D) or 60 s (E) of continuous yellow light. *, # and ‡ indicate statistically significant differences. *: repeated measures ANOVA with Tukey's post-hoc test. ‡: repeated measures ANOVA with Bonferroni post-hoc test (post-light vs pre-light specifically). #: unpaired Student's t-test (compared to light periods of control group). See further in Table 2 and Results. Whiskers: SD.

When yellow light was applied to the NpHR3.0-expressing slices for 30 or 60 seconds, the mean number of bursts per 30 s period significantly decreased compared to respective pre- and post-light periods, as shown in Figure 1 D & E, with data summarized in Table 2. For NpHR3.0-transduced non-epileptic animals (Naïve group), burst frequency was reduced by 85% compared to pre-light levels with 30 s light exposure (repeated measures ANOVA, $F_{2,16} = 76.4$, $P < 0.001$, with Tukey's posthoc-test: $P < 0.001$). With a 60 s light period, burst frequency was reduced by 82% and 57% (for 0-30 and 30-60 s periods, respectively) compared to pre-light levels (repeated measures ANOVA, $F_{3,24} = 42.3$, $P < 0.001$, with Tukey's posthoc-test: $P < 0.001$ & $P < 0.001$). Additionally, we observed an increase of burst frequency in the post-light period by 19% and 38% (30 s and 60 s stimulation, respectively) when compared to pre-light period (Bonferroni's posthoc test, $P < 0.05$ and $P = 0.004$).

To explore whether transgene NpHR3.0 could also attenuate bursting activity in hyperexcitable epileptic tissue, where excitability of CA3 pyramidal cells is increased (Queiroz and Mello, 2007), and axonal sprouting enhance excitatory interconnectivity between principle neurons, hippocampal slices from kainic acid (KA)-treated animals were used. Intraperitoneal injection of KA leads to acute status epilepticus (SE), occurrence of post-SE spontaneous seizures and later on to chronic epilepsy. In this model, extensive neuronal cell loss, gliosis and mossy fiber sprouting in the dentate gyrus is routinely observed (Cantallops and Routtenberg, 2000; Royle et al., 1999), resembling changes seen in patients with temporal lobe epilepsy (Pitkänen et al., 2006; Wieser and ILAE, 2004). To confirm that our KA-treated animals also undergo such characteristic structural network reorganizations, we performed an immunohistochemical evaluation of mossy fiber sprouting by staining slices against

Figure 2

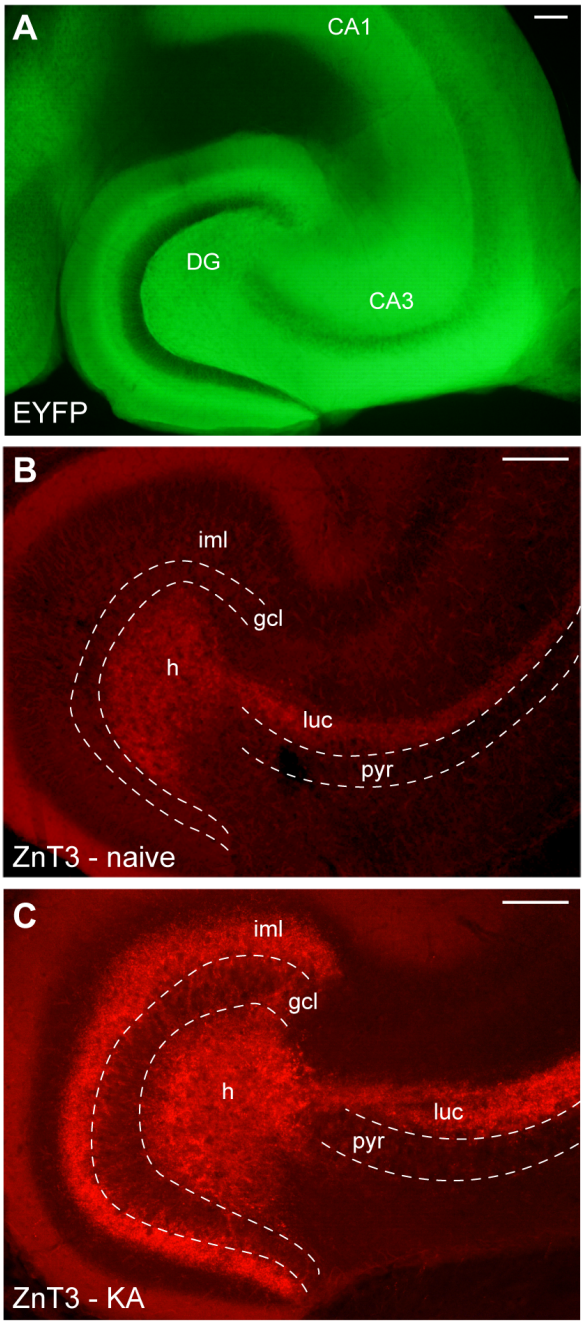

Figure 2 NpHR3.0 expression in the hippocampus of AAV-hSyn-eNpHR3.0-eYFP-injected mice, and mossy fiber sprouting in KA-injected mice, in acute slices used for *in vitro* electrophysiology. **A.** NpHR3.0-eYFP fusion protein visualized by GFP antibody in a horizontal slice representative of *in vitro* trials. **B & C**. Staining with ZnT3 antibody reveals mossy fiber sprouting only in KA-injected mice (**C**). DG: dentate gyrus, gcl: granule cell layer, h: hilus, iml: inner molecular layer, luc: stratum lucidum, pyr: pyramidal cell layer. Scale bars: 200 µm.

Table 2. Attenuation of epileptiform bursting frequency during light in NpHR3.0-expressing acute brain slices *in vitro*. All values are mean (SD) bursts per 30 s period, normalised to the mean value of the pre-light period. See also Figure 1 D & E.

	Naïve NpHR (n=9)				KA NpHR (n=8)				Control (n=6)	
	Pre	Light 0-30	Light 30-60	Post	Pre	Light 0-30	Light 30-60	Post	Light 0-30	Light 30-60
30s light	1 (0.24)	0.15 (0.17)	-	1.19 (0.39)	1 (0.23)	0.13 (0.18)	-	1.19 (0.44)	1.05 (0.38)	-
60s light	1 (0.32)	0.18 (0.25)	0.42 (0.39)	1.38 (0.53)	1 (0.16)	0.16 (0.18)	0.34 (0.28)	1.36 (0.45)	0.96 (0.34)	1.01 (0.33)

ZnT3 (Chi et al., 2008). Representative slices from a KA treated and a normal animal are shown in Fig. 2B & C, demonstrating substantial mossy fiber sprouting in the inner molecular layer of the dentate gyrus in KA treated animals.

Similar to NpHR3.0-transduced non-epileptic animals, hippocampal slices obtained from NpHR3.0-transduced KA-treated animals showed attenuation of epileptiform bursting activity during the yellow light exposure (Fig. 1 D & E, KA group; Table 2). With a 30 s light period, burst frequency was reduced by 87% compared to pre-light (repeated measures ANOVA, $F_{2,14}$ = 37.7, P < 0.001, with Tukey's posthoc-test: P < 0.001). With 60 s light the reduction was 84% and 66% of pre-light levels; 0-30 and 30-60 s periods, respectively (repeated measures ANOVA, $F_{3,21}$ = 28.7, P < 0.001, with Tukey's post-test: P < 0.001 & P = 0.001). A statistically significant increase of bursting frequency in the post-light period was detected for the 60 s light stimulation (36% increase, P = 0.025, Bonferroni's posthoc test).

In contrast to the NpHR3.0-transduced groups (Naïve and KA), the control group was unaffected by light, indicating that the burst reduction in the transduced groups was indeed mediated by NpHR3.0 activation (Fig. 1 D & E, Control group; Table 2). During 30s light exposure, the number of bursts was 86% lower in the Naïve group compared to control (unpaired two-tailed Student's t-test, t_{13}= 5.4, P = 0.002, with Welch's correction for unequal variances) and, with 60 s light, 81% and 57% lower compared to control group (for 0-30 & 30-60 s periods, respectively, one-way ANOVA, $F_{3,26}$= 10.8, P < 0.001, with Tukey's posthoc-test: P < 0.001 & P = 0.007). Similarly, compared to control group, the KA group displayed greatly reduced burst frequency during light: 88% reduction with 30 s light stimulation (unpaired two-tailed Student's t-test, t_{12}= 6.0, P < 0.001) and 83% and 66% reduction with 60 s light (0-30 & 30-60 s periods, respectively, one-way ANOVA $F_{3,24}$= 16.1, P < 0.001, with Tukey's posthoc-test: P < 0.001 & P < 0.001).

In addition, the individual burst durations during light were significantly decreased for both Naïve and KA groups. In slices where bursting was not completely suppressed (5 out of 9 and 6 out of 8 for Naïve and KA groups, respectively, table 3) the individual burst duration was reduced by 23 % during light in the Naïve group compared to pre-light (paired two-tailed Student's t-test, t_5= 2.6, P = 0.046) and by 30 % in the KA group (paired two-tailed Student's t-test, t_6= 5.1, P = 0.002). The individual burst duration was unaltered in the control group (paired two-tailed Student's t-test, t_6= 0.57, P = 0.59). Similarly, total time of bursting per minute was markedly lower during light compared to pre- and post-periods for both Naïve and KA groups (table 3) (repeated measures ANOVA, Naïve: $F_{2,10}$ = 28.2, P < 0.001, with Tukey's post-test: P < 0.001 and KA: $F_{2,14}$ = 63.7, P < 0.001, with Tukey's post-test: P < 0.001), while control group was unaffected (repeated measures ANOVA, $F_{2,10}$ = 1.9, P = 0.2). The duration of the first burst immediately after light was switched off was increased in the Naïve group vs the average pre-light burst (table 3) (paired two-tailed Student's t-test, t_7= 3.7, P = 0.0072). In the KA injected animals, the increase did not reach statistical significance (paired

Table 3. Reduction of individual burst duration during light in NpHR3.0 expressing acute brain slices *in vitro*. For this data, 30 s and 60 s light stimulation periods were added together. All values mean (SD).

Individual burst durations (ms)								
Naive	(n=5)		KA	(n=6)		Control	(n=6)	
Pre	Light		Pre	Light		Pre	Light	
70 (29)	54 (33)		83 (26)	58 (27)		88 (29)	87 (28)	
Total time of bursting per minute (s)								
Naive	(n=5)		KA	(n=6)		Control	(n=6)	
Pre	Light	Post	Pre	Light	Post	Pre	Light	Post
2.1 (0.9)	0.4 (0.3)	2.6 (1.1)	1.8 (0.5)	0.3 (0.2)	1.9 (0.7)	1.7 (0.8)	1.7 (0.7)	1.7 (0.8)
Duration of first burst after light (ms)								
Naive	(n=9)		KA	(n=8)		Control	(n=6)	
Pre	First post		Pre	First post		Pre	First post	
70 (25)	214 (216)		74 (17)	130 (72)		88 (29)	90 (27)	

two-tailed Student's t-test, t_7= 2.1, P = 0.07). In the control group, the first burst after light was unaltered (paired two-tailed Student's t-test, t_5= 0.49, P = 0.65).

Taken together, these data suggest that optogenetic silencing of principal neurons is able to attenuate epileptiform bursting when inhibitory circuits are disconnected from the principal cells in acute brain slices from both normal and epileptic animals.

Epileptiform bursting in vivo

Although *in vitro* slice studies provide a good estimate of neurophysiological processes, the more complex interconnectivity of the intact brain needs to be taken in account to validate the *in vitro* data. Therefore, we next asked whether *in vivo* epileptiform activity induced by compromised inhibitory transmission could be affected by a similar optogenetic approach. Because of the *in vitro* data showing similar effect of optogenetics on normal and epileptic tissue, we focused our *in vivo* studies on non-epileptic NpHR3.0-transfected animals. Instead of PTX we used the competitive $GABA_A$ receptor antagonist Bicuculline Methiodide (BM), as it has been shown that PTX displays slower induction of bursting *in vivo* (Veliskova et al., 1990).

Using an optrode (Gradinaru et al., 2007) customized with a microcapillary (Fig. 3A), we infused BM directly into the area of the optrode tip, with the fiber end placed in the CA1/CA2 area of the hippocampus (Fig. 3B) and the electrode and capillary tip further extending into the ventral CA1/CA3 or DG. The optrode localisation was well within the

Figure 3

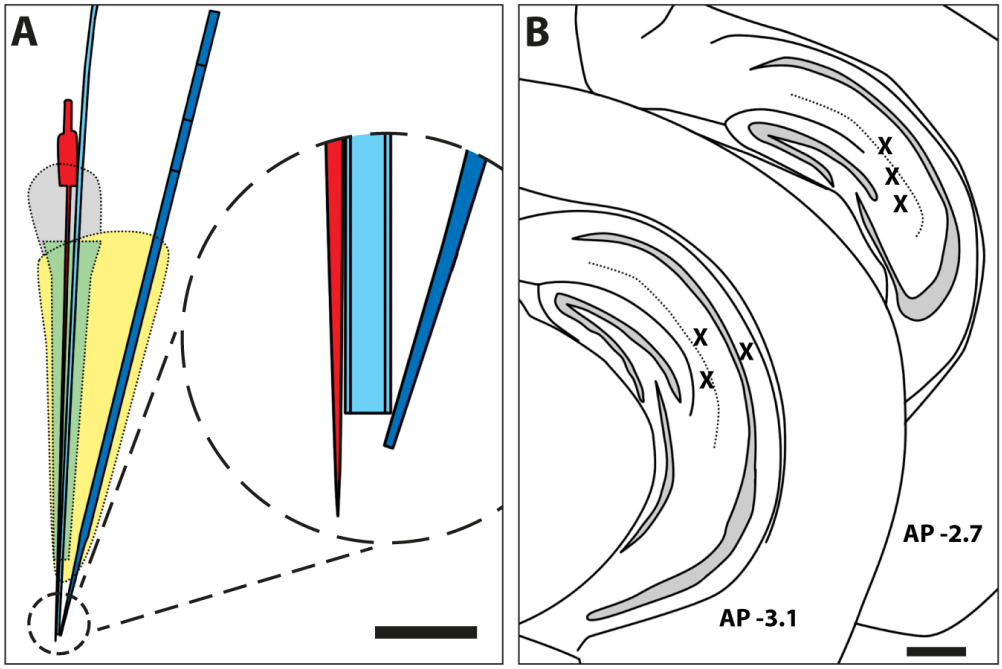

Figure 3 Chemical optrode: combined optrode and glass capillary for fluid injection. **A.** Schematic figure of the chemical optrode. Electrode in red, optic fiber in light blue, injection capillary in dark blue. Structural components in green, yellow & gray. Scalebar: 10 mm for whole optrode, 0.5 mm for inset. **B.** Optrode placement in the NpHR3.0 group *in vivo*. Each cross represents the position of the end of the optic fiber, placed in two coronal planes corresponding to their final location in each animal as judged by damage in brain slices. Note that the electrode tip protrudes further ventrally by ~0.5 mm. Scalebar: 0.5 mm.

area of the transgene expression in the hippocampi (compare Fig. 3B and 4A & B). Within minutes, the BM injection induced a stable low frequency bursting recorded by the optrode, with a mean frequency of 5.1 (0.95) bursts min^{-1}. In some animals spontaneous multi-unit activity (neuronal action potentials) could be recorded by the optrode, prior to BM injection. This multi-unit activity was readily inhibited by yellow (593 nm) light (Fig. 4 E) in NpHR3.0-tranduced animals. The effect of light could also be seen as a large deflection in the LFP in all the NpHR3.0-tranduced animals at light onset (Fig. 5A).

A typical BM-induced epileptic burst consisted of a large initial spike followed by a short wave of variable length (Fig 5A), with a mean duration of 0.56 s (0.19) (n = 6 animals). The 40 second light exposure through the optrode reduced the mean number of bursts compared to pre- and post-light periods in the NpHR3.0-transduced animals by 17 % and 21%, respectively (Fig 5B); 2.8 (0.76) vs. 3.3 (0.59) and 3.5 (0.71) bursts per period (repeated measures ANOVA, $F_{2,10} = 11.1$, $P = 0.003$, with Tukey's post-test: $P = 0.016$, $P = 0.003$). The mean bursting was also attenuated by 22% compared to the control group (NpHR3.0-negative) during the light period, normalized to the pre-light period in each group (Fig. 5 C); trial light-on vs. control light-on: 0.83 (0.10) vs. 1.05 (0.12) (unpaired two-tailed Student's t-test, $t_{10} = 3.6$, $P = 0.005$). Individual burst duration was not affected by light; pre 0.55 (0.21) s, light 0.57 (0.21) s, post 0.57 (0.18) s (repeated measures ANOVA, $F_{2,10} = 0.97$, $P = 0.4$).

We also observed an increased probability of bursting right after the light switch-off (Fig. 5A & D), closely resembling the *in vitro* situation (Fig. 1). Sorting the bursts in 4 s bins, the mean number of bursts in the first bin post-light was more than twice as high compared to the last bin pre-light (Fig 5D); 6.5 (1.6) vs 3.0 (2.8) (paired two-tailed Student's t-test, $t_5 = 3.1$, $P = 0.03$). In the control group, no such increase was observed;

Figure 4

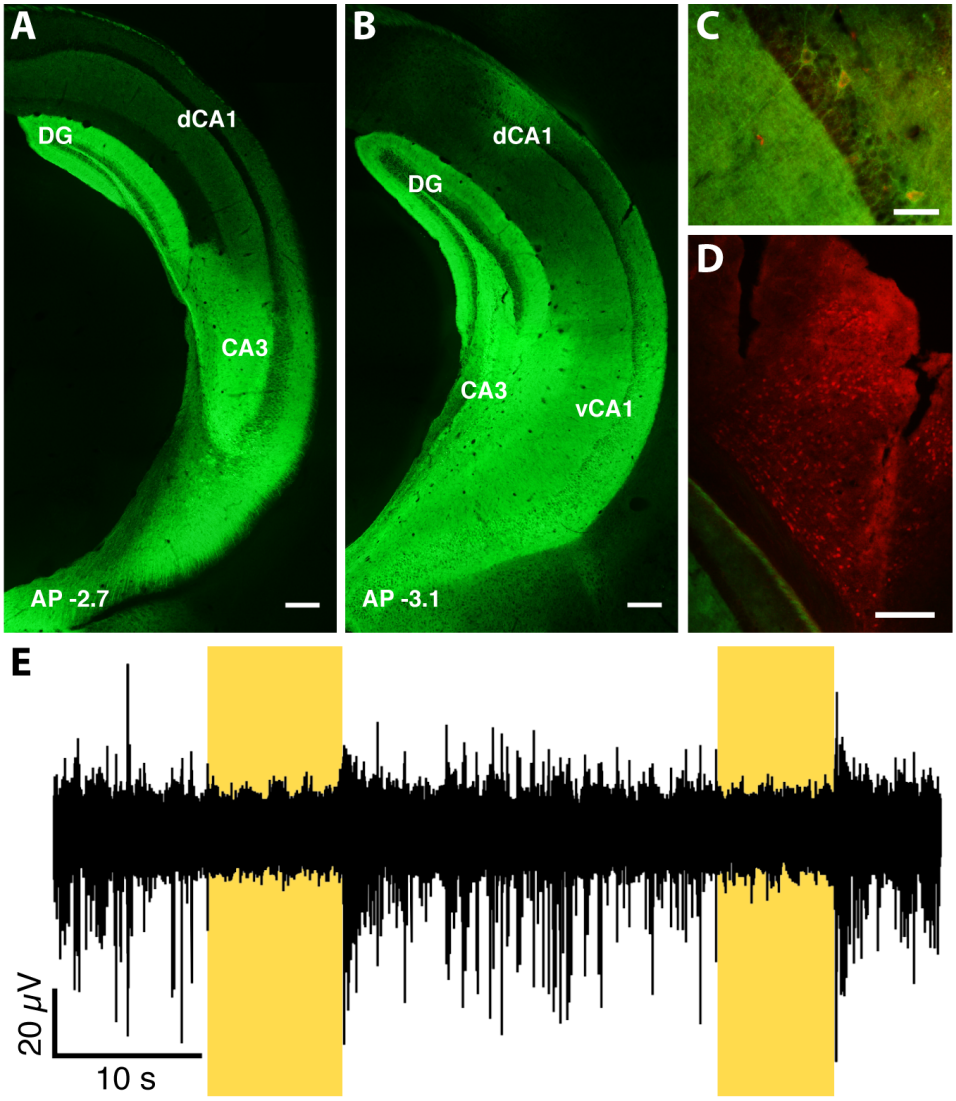

Figure 4 NpHR3.0 expression and spontaneous activity inhibition in the hippocampus of mice of the *in vivo* trial. **A & B.** Composite images of NpHR3.0-eYFP fusion protein autofluorescence in two coronal planes of a trial mouse, corresponding to the optrode locations in the six trial animals (see Fig. 3B). **C.** Pyramidal cells in the ventral CA1 expressing NpHR3.0-eYFP (green) displaying uptake of biocytin (Cy3 staining, red), indicating the diffusion of BM-solution during experiment. **D.** Overview of cortical area in a trial mouse, indicating leakage of BM-solution into the cortex along the optrode/capillary tract. **E.** 60 s trace of spontaneous multiunit activity in the CA2/CA3 area of a sedated mouse expressing NpHR3.0, with two periods of 593 nm light inhibiting the activity (yellow areas). Scalebars: A, B & D: 200 μm, C: 50 μm. DG: dentate gyrus, dCA1: dorsal CA1, vCA1: ventral CA1.

Figure 5

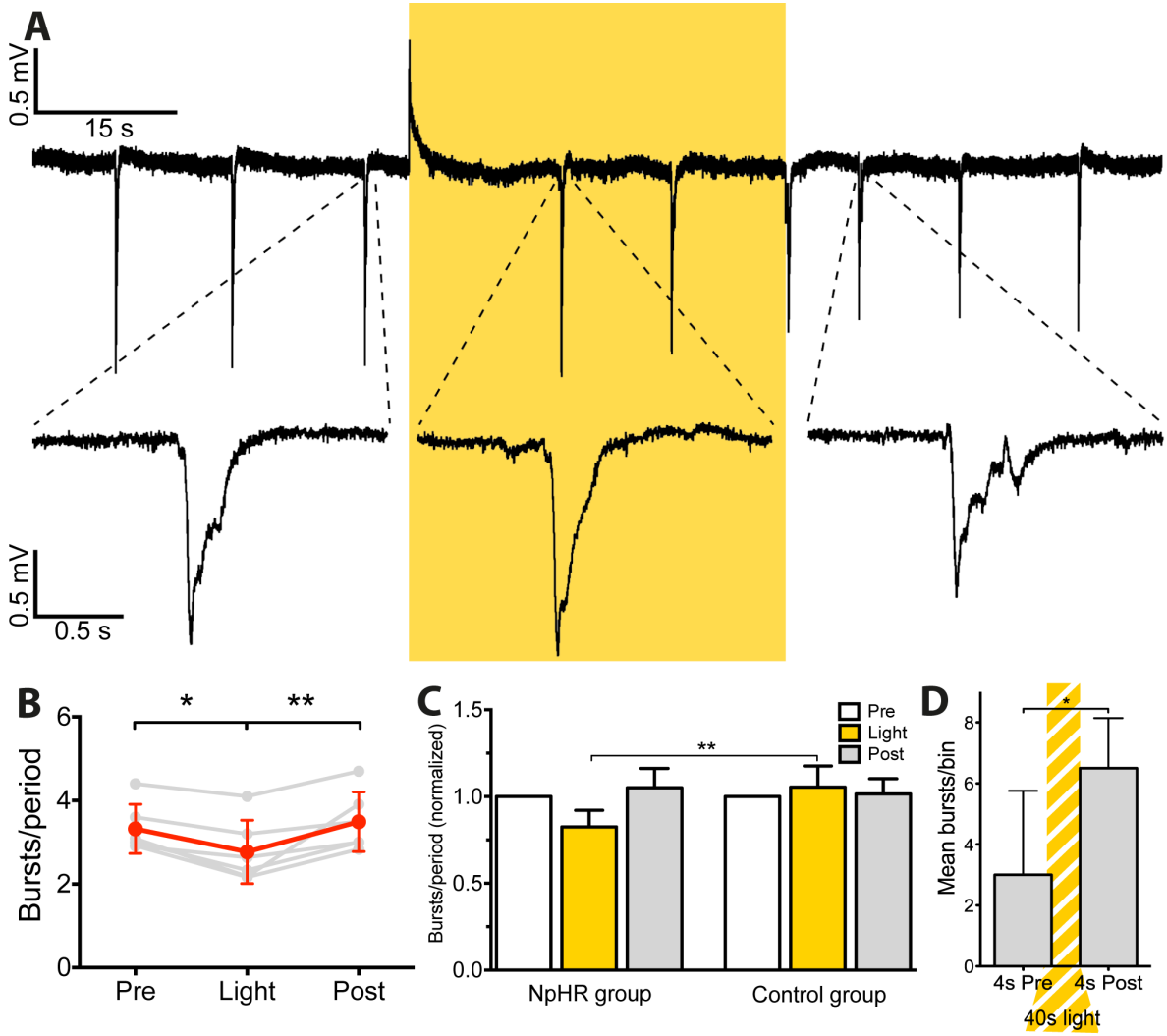

Figure 5 Bicuculline methiodide induced bursting in the mouse hippocampus can be reduced by optogenetic treatment *in vivo*. **A.** Representative trace of BM-induced bursting from one animal in the NpHR3.0-expressing group. Top: a continuous 120 s trace with a 40 s period of 593 nm light outlined by the yellow box. Bottom: insets of bursts from pre-, light and post-light periods as indicated by the dashed lines, with common scale bar. **B.** The mean number of bursts in 40 s periods in the NpHR-transduced group (red plot, n=6) was reduced during light compared to both pre-light and post-light (repeated measures ANOVA, Tukey's post-test: pre vs light *p<0.05, light vs post **p<0.01). Grey plots: individual animal means. **C.** To allow direct comparison to control animals, bursting was normalized to the mean number of bursts pre-light (40s periods) in each animal individually, to account for variability of burst frequency. The mean of bursting during light was significantly different between the NpHR3.0-positive group and non-expressing control group (n=6) (unpaired t-test, two-tailed, **p=0.005). **D.** In the NpHR group there was a marked increase of bursts occurring in the first 4 seconds post light compared to the last 4 seconds pre light (paired t-test, two-tailed, *p=0.03). Whiskers: SD.

pre-light vs. post-light: 4.3 (4.4) vs. 3.3 (2.2) (paired two-tailed Student's t-test, t_5 = 1.0, P = 0.36).

The BM solution contained biocytin to determine diffusion distance of the infused BM solution. In post mortem histology biocytin could be detected throughout the ventral hippocampus (Figure 4 C), i.e. 1.8 mm DV and 1.3 mm AP, 1.3 mm ML around the injection site. However, biocytin staining was also observed along the optrode insertion track in the cortex (Figure 4 D).

Discussion

Here we show for the first time that when hyperexcitability in the hippocampus is induced by compromised inhibitory drive onto the principal neurons, optogenetic hyperpolarization of principal cells attenuates epileptiform activity both *in vitro* and *in vivo*.

Optogenetic silencing of principal neurons in organotypic hippocampal cultures has been shown to suppress stimulation-induced bursting (Tonnesen et al., 2009), with silencing achieved by yellow light illumination of slices selectively expressing NpHR2.0 under the CaMKIIa promoter in principal neurons. Likewise, when NpHR2.0 was expressed in principal cells of neocortex, yellow light illumination attenuated epileptiform events induced by tetanus toxin (Wykes et al., 2012). In these studies epileptiform activity was induced either with intact inhibitory transmission (in the former case) or with only transient impairement of GABA release from inhibitory interneurons (Empson et al., 1993). GABAergic interneurons (e.g. PV-, or SOM-expressing ones) may contribute to hypersynchronized epileptiform activity and promote seizures (Avoli and de Curtis, 2011; Isomura et al., 2008). However, it is well

known that pharmacological disconnection of inhibitory neurotransmission from principal cells and inhibitory interneurons using $GABA_A$ receptor blockers, such as PTX or bicuculine, can induce epileptiform activity both *in vitro* and *in vivo* (de Curtis and Avanzini, 2001). In these situations, epileptiform activity is most likely driven predominantly by principal cells through their excitatory network connections (de Curtis et al., 1999; Hwa et al., 1991; Miles and Wong, 1983; Traub et al., 1993). Our data show that hyperpolarization of principal neurons by light-activated NpHR3.0 effectively suppress such epileptiform activity *in vitro* and significantly attenuates it *in vivo*.

Inhibition of epileptiform bursts by NpHR-based optogenetics *in vivo* was not of the same magnitude as *in vitro* in acute slices. While there is almost complete burst suppression during the first 30 s of light illumination *in vitro*, the reduction in bursting is moderate *in vivo* (17%). Several factors could contribute to this difference. The most probable explanation is the diffusion of the intrahippocampally injected BM to a large volume of the hippocampus, as assessed by co-injected biocytin staining in the post-mortem tissue. Given the estimated dispersion of 593 nm light in brain tissue (Chow et al., 2010), the zone illuminated with sufficient light energy for NpHR3.0 activation would extend below and sideways of the fiber 0.6-0.8 mm. At the same time, biocytin staining was seen in the entire ventral hippocampus (1.3 mm or more around the injection site), as well as in the cortex. This widespread diffusion of bicuculline would affect the hippocampal tissue outside the reach of the optogenetic treatment, thereby allowing the epileptiform activity to partially escape optogenetic control.

Both *in vitro* and *in vivo,* we observed increased burst generation by light switch-off. It has been shown previously that after NpHR3.0 silencing in CA1 and CA3, the probability of action potential generation is increased due to accumulating intracellular Cl^- levels that reverse $GABA_A$ receptor potentials from hyperpolarizing to

depolarizing (Raimondo et al., 2012). However, in our study $GABA_A$ receptors were blocked by PTX and BM during the *in vitro* and *in vivo* experiments, respectively, and could not account for this phenomenon. Instead, it is more likely that T-type Ca^{2+} and/or hyperpolarization-activated cyclic nucleotide-gated (HCN) channels affected by the prolonged light-induced hyperpolarizations could trigger the rebound action potentials in the principal cells, and thereby generate bursts at the switch-off of the light (Santoro et al., 2000; Siwek et al., 2012). Rebound bursting may impose a risk of triggering epileptiform activity at the light termination and therefore needs to be accounted for when designing seizure-suppressant paradigms using an NpHR-based optogenetic approach. For example, slowly attenuating light instead of abrupt switching-off could be considered, or pulsed light, which was shown to not induce any rebound discharges post-light (Krook-Magnuson et al., 2013). In any case, as shown previously (Tonnesen et al., 2009), NpHR-induced hyperpolarization triggers rebound action potentials to a similar extent as electrical hyperpolarization, i.e. the rebound is not exacerbated by NpHR expression *per se*. It should be noted that the hSyn promoter drives expression of NpHR3.0 also in interneurons, leading to their hyperpolarization and reduced GABA release during light exposure. Although such a scenario was favorable to adress the objectives of the present study, it may not be desirable in clinical applications, since hyperpolarization of remaining interneurons in the epileptic focus could induce a catastrophic loss of inhibition that may not be overcome by hyperpolarization of principal neurons by Halorhodopsin. Specific promoters for principal neurons, such as CaMKIIα, may be preferable in this case.

In conclusion, our data show that epileptiform activity, generated in hippocampal circuits by disconnected inhibition, can be readily controlled by NpHR-based

hyperpolarization of principal neurons and underlines a potential use of such optogenetic strategy as an alternative treatment for epileptic seizures, particularly in pharmacoresistant epilepsy cases where inhibitory transmission is often severely compromised. However, in those cases when seizures are not associated with impaired inhibition, microenvironmental alterations of chloride homeostasis by NpHR activation should be taken in account, since it may convert GABAergic inhibition into excitation by reversing hyperpolarizing potentials generated by $GABA_A$ receptors into depolarizations (Raimondo et al., 2012), potentially leading to excessive activation of the principal neurons. Taken together, our data encourage further investigations on various possibilities for normalizing neuronal circuits in the conditions of pathological hyperexcitability and hypersynchronized activity by using optogenetic strategies (see e.g. (Krook-Magnuson et al., 2013; Paz et al., 2013)) as an alternative to traditional pharmacological or electrical treatments, which often fail as a therapy in patients.

References

Avoli, M., de Curtis, M., 2011. GABAergic synchronization in the limbic system and its role in the generation of epileptiform activity. Prog Neurobiol. 95**,** 104-32.

Bogen, I. L., et al., 2009. The importance of synapsin I and II for neurotransmitter levels and vesicular storage in cholinergic, glutamatergic and GABAergic nerve terminals. Neurochem Int. 55**,** 13-21.

Cantallops, I., Routtenberg, A., 2000. Kainic acid induction of mossy fiber sprouting: dependence on mouse strain. Hippocampus. 10**,** 269-73.

Cardin, J. A., et al., 2010. Targeted optogenetic stimulation and recording of neurons in vivo using cell-type-specific expression of Channelrhodopsin-2. Nat Protoc. 5**,** 247-54.

Chi, Z. H., et al., 2008. Zinc transporter 3 immunohistochemical tracing of sprouting mossy fibres. Neurochem Int. 52**,** 1305-9.

Chow, B. Y., et al., 2010. High-performance genetically targetable optical neural silencing by light-driven proton pumps. Nature. 463**,** 98-102.

de Curtis, M., Avanzini, G., 2001. Interictal spikes in focal epileptogenesis. Prog Neurobiol. 63**,** 541-67.

de Curtis, M., et al., 1999. Cellular mechanisms underlying spontaneous interictal spikes in an acute model of focal cortical epileptogenesis. Neuroscience. 88**,** 107-17.

de Lanerolle, N. C., et al., 1989. Hippocampal interneuron loss and plasticity in human temporal lobe epilepsy. Brain Res. 495**,** 387-95.

Duncan, J. S., et al., 2006. Adult epilepsy. Lancet. 367**,** 1087-100.

Empson, R. M., et al., 1993. Injection of tetanus toxin into the neocortex elicits persistent epileptiform activity but only transient impairment of GABA release. Neuroscience. 57**,** 235-9.

Engel, J., Jr., 2001. Mesial temporal lobe epilepsy: what have we learned? Neuroscientist. 7**,** 340-52.

Gradinaru, V., et al., 2007. Targeting and readout strategies for fast optical neural control in vitro and in vivo. J Neurosci. 27**,** 14231-8.

Gradinaru, V., et al., 2010. Molecular and cellular approaches for diversifying and extending optogenetics. Cell. 141**,** 154-65.

Hwa, G. G., et al., 1991. Bicuculline-induced epileptogenesis in the human neocortex maintained in vitro. Exp Brain Res. 83**,** 329-39.

Isomura, Y., et al., 2008. A network mechanism underlying hippocampal seizure-like synchronous oscillations. Neurosci Res. 61, 227-33.

Krook-Magnuson, E., et al., 2013. On-demand optogenetic control of spontaneous seizures in temporal lobe epilepsy. Nat Commun. 4, 1376.

Kumar, S. S., Buckmaster, P. S., 2006. Hyperexcitability, interneurons, and loss of GABAergic synapses in entorhinal cortex in a model of temporal lobe epilepsy. J Neurosci. 26, 4613-23.

Ledri, M., et al., 2012. Altered profile of basket cell afferent synapses in hyper-excitable dentate gyrus revealed by optogenetic and two-pathway stimulations. Eur J Neurosci. 36, 1971-83.

Malmgren, K., Thom, M., 2012. Hippocampal sclerosis--origins and imaging. Epilepsia. 53 Suppl 4, 19-33.

Miles, R., Wong, R. K., 1983. Single neurones can initiate synchronized population discharge in the hippocampus. Nature. 306, 371-3.

Morimoto, K., 1989. Seizure-triggering mechanisms in the kindling model of epilepsy: collapse of GABA-mediated inhibition and activation of NMDA receptors. Neurosci Biobehav Rev. 13, 253-60.

Morimoto, K., Goddard, G. V., 1986. Kindling induced changes in EEG recorded during stimulation from the site of stimulation: collapse of GABA-mediated inhibition and onset of rhythmic synchronous burst. Exp Neurol. 94, 571-84.

Paz, J. T., et al., 2013. Closed-loop optogenetic control of thalamus as a tool for interrupting seizures after cortical injury. Nat Neurosci. 16, 64-70.

Piredda, S., et al., 1985. Intracerebral site of convulsant action of bicuculline. Life Sci. 36, 1295-8.

Pitkänen, A., et al., 2006. Models of seizures and epilepsy. Elsevier Academic, Amsterdam ; Oxford.

Queiroz, C. M., Mello, L. E., 2007. Synaptic plasticity of the CA3 commissural projection in epileptic rats: an in vivo electrophysiological study. Eur J Neurosci. 25, 3071-9.

Racine, R. J., 1972. Modification of seizure activity by electrical stimulation. II. Motor seizure. Electroencephalogr Clin Neurophysiol. 32, 281-94.

Raimondo, J. V., et al., 2012. Optogenetic silencing strategies differ in their effects on inhibitory synaptic transmission. Nat Neurosci. 15, 1102-4.

Royle, S. J., et al., 1999. Behavioural analysis and susceptibility to CNS injury of four inbred strains of mice. Brain Res. 816, 337-49.

Sander, J. W., 2003. The epidemiology of epilepsy revisited. Curr Opin Neurol. 16, 165-70.

Santoro, B., et al., 2000. Molecular and functional heterogeneity of hyperpolarization-activated pacemaker channels in the mouse CNS. J Neurosci. 20, 5264-75.

Siwek, M., et al., 2012. Voltage-gated Ca(2+) channel mediated Ca(2+) influx in epileptogenesis. Adv Exp Med Biol. 740, 1219-47.

Strombom, U., et al., 1979. Regulation of the state of phosphorylation of specific neuronal proteins in mouse brain by in vivo administration of anesthetic and convulsant agents. Proc Natl Acad Sci U S A. 76, 4687-90.

Tonnesen, J., et al., 2009. Optogenetic control of epileptiform activity. Proc Natl Acad Sci U S A. 106, 12162-7.

Traub, R. D., Jefferys, J. G., 1994. Simulations of epileptiform activity in the hippocampal CA3 region in vitro. Hippocampus. 4, 281-5.

Traub, R. D., et al., 1993. Synaptic and intrinsic conductances shape picrotoxin-induced synchronized after-discharges in the guinea-pig hippocampal slice. J Physiol. 461, 525-47.

Veliskova, J., et al., 1990. Ketamine suppresses both bicuculline- and picrotoxin-induced generalized tonic-clonic seizures during ontogenesis. Pharmacol Biochem Behav. 37, 667-74.

Wieser, H. G., ILAE, C. o. N. o. E., 2004. ILAE Commission Report. Mesial temporal lobe epilepsy with hippocampal sclerosis. Epilepsia. 45, 695-714.

Wykes, R. C., et al., 2012. Optogenetic and potassium channel gene therapy in a rodent model of focal neocortical epilepsy. Sci Transl Med. 4, 161ra152.

Zhang, F., et al., 2007. Multimodal fast optical interrogation of neural circuitry. Nature. 446, 633-9.

Zhang, W., Buckmaster, P. S., 2009. Dysfunction of the dentate basket cell circuit in a rat model of temporal lobe epilepsy. J Neurosci. 29, 7846-56.